ResearchGate

See discussions, stats, and author profiles for this publication at: https://www.researchgate.net/publication/231695829

Effect of Hydrogen Bonding Strength on the Microstructure and Crystallization Behavior of Crystalline Polymer Blends

ARTICLE *in* MACROMOLECULES · JULY 2003

Impact Factor: 5.8 · DOI: 10.1021/ma034695a

CITATIONS
60

READS
16

3 AUTHORS, INCLUDING:

Shiao-Wei Kuo
National Sun Yat-sen University
267 PUBLICATIONS **5,589** CITATIONS

SEE PROFILE

Available from: Shiao-Wei Kuo
Retrieved on: 26 January 2016

Effect of Hydrogen Bonding Strength on the Microstructure and Crystallization Behavior of Crystalline Polymer Blends

Shiao-Wei Kuo, Shih-Chi Chan, and Feng-Chih Chang*

Institute of Applied Chemistry, National Chiao Tung University, Hsin Chu, Taiwan

Received May 26, 2003; Revised Manuscript Received July 7, 2003

ABSTRACT: Combinations of differential scanning calorimetry, Fourier transform infrared spectroscopy, optical microscopy, and small-angle X-ray scattering were used to investigate the influence of hydrogen bonding strength on the crystallization kinetics and morphologies in poly(ϵ-caprolactone) (PCL) blends with three different well-known hydrogen bond donating polymers, i.e., phenolic, poly(vinylphenol) (PVPh), and phenoxy. The strength of the intercomponent interactions in the blend system depends on the hydrogen bond donor group and occurs, based on the Painter−Coleman association model, in the order phenolic/PCL > PVPh/PCL > phenoxy/PCL. Significantly reduced overall crystallization kinetics and crystal growth rate in PCL crystalline phase were also in the order phenolic/PCL > PVPh/PCL > phenoxy/PCL, which is consistent with the relative strengths of their intermolecular hydrogen bonding. Our experimental findings show that the hydrogen bonding strength has a greater effect on the rate of crystallization than does the influence of the blend's glass transition temperature, which is related to its chain mobility. In addition, values of the surface free energy of chain folding and crystalline thickness in PCL blends depend strongly on the relative ratio of the interassociation equilibrium constant and the self-association equilibrium constant (K_A/K_B). In phenolic/PCL and PVPh/PCL blends, the values of the surface free energies of chain folding in the PCL crystalline phase are increased with an increase in the content of the hydrogen bond donating polymer since the K_A is greater than the K_B in these two blend systems. In contrast, in the phenoxy/PCL blend system, the smaller K_A relative to the K_B induces a smaller value for the surface free energy of chain folding than that of pure PCL. Various miscible crystalline/amorphous binary polymer blends exhibiting either strong hydrogen bonding or weak interactions are also reviewed.

Introduction

Crystalline polymers are ubiquitous ranging from the commodity polyethylene to high-performance engineering resins, such as nylons and poly(ether ether ketone). The crystallization behavior of polyethylene has been discussed widely by many authors.[1−5] Within the polyethylene's main chains, however, there exists no specific interactions. Therefore, it is of quite some interest to study crystallization in polymer blends with regard to intermolecular interaction, such as hydrogen bonding and dipole−dipole interactions. Relative to neat crystalline materials, the crystalline microstructures and crystallization kinetics of polymer blends containing crystalline polymers are less well understood because of their inherent complexities. As a result, it is necessary to establish a general principle for predicting the nature of polymer crystallization in polymer blends.

On the basis of the crystallizability of the constituents, binary crystalline polymer blends can be categorized into crystalline/amorphous and crystalline/crystalline systems. Crystalline/amorphous binary polymer blends are more widely studied because of their simpler crystalline phase relative to crystalline/crystalline ones.[6−19] Various morphologies have been created depending upon the distance of segregation in crystallization of a melt-miscible crystalline/amorphous blend. These segregation types include interlamellar, interfibriallar, and interspherulitic segregations.[6,7] These morphology patterns represent the diluent dispersion from the nanoscopic scale, for interlamellar segregation, to the micrometer scale, for interspherulitic segregation. Keith and Padden[20] have suggested that the distance over which an amorphous impurity may be segregated is determined by the interplay between the diffusion coefficient (D) of impurity molecules and the crystal growth rate (G). If the diffusion of diluent is relatively slow compared to the crystal growth rate, the diluent may become trapped inside the interlamellar segregation. On the contrary, if diluent diffusion is faster, interfibriallar or interspherulitic segregations are generated. This result is related to a parameter δ, which is defined as the ratio of the diffusion coefficient of the impurity in the melt to the spherulitic growth rate ($\delta = D/G$). The parameter δ has the unit of length and provides a qualitative measure of the segregation distance, which depends on the composition, temperature, molecular weight, and polymer−polymer interactions within the polymer blend.

In addition, the crystallization kinetics, the surface free energy of chain folding, and the thickness of crystalline phase in miscible polymer blends through hydrogen bonding have received relatively less attention.[21,22] In general, the crystallization kinetics and microstructures of a crystalline blend depend on the effects of the glass transition temperature and intermolecular interactions of the diluent amorphous phase. In a previous study, Runt et al.[21] found that blends of poly(ethylene oxide) (PEO) with amorphous polymeric diluents exhibited either relatively weak interactions, including poly(vinyl acetate) (PVAc) and poly(methyl methacrylate) (PMMA), or strong hydrogen bonding interactions, including ethylene-*co*-methacrylic acid55 (EMAA55, 55 wt % of MAA) copolymer and styrene-*co*-hydroxystyrene50 (SHS50, 50 wt % of hydroxystyrene) copolymer. At a given crystallization temperature (T_c), spherulite growth rates for blends with strongly hydro-

* To whom corresponding should be addressed: e-mail changfc@cc.nctu.edu.tw; tel 886-3-5727077; fax 886-3-5719507.

10.1021/ma034695a CCC: $25.00 © 2003 American Chemical Society
Published on Web 08/01/2003

gen bonding polymers are considerably lower than those with weakly interacting polymers with comparable glass transition temperature, e.g., comparison between the PMMA/PEO and SHS50/PEO or PVAc/PEO and EMAA/PEO blend systems. Furthermore, a study of the spherulite radius of PEO in blends with the strongly interacting EMAA55 and SHS50 showed that the SHS50/PEO blend has lower crystallization kinetics than EMAA50/PEO blend because of the higher glass transition temperature of SHS50. However, the different intermolecular hydrogen bonding strengths in the SHS50/PEO and EMAA50/PEO blends were not considered. The main purposes of this work was to study the crystallization kinetics, surface free energies of chain folding, and crystal thickness with respect to the different hydrogen bonding strengths in crystalline polymer blends.

A commonly employed component in most crystalline miscible blends is a polyester, such as poly(ϵ-caprolactone) (PCL). PCL is a highly crystalline polymer that is miscible with several amorphous polymers through specific interactions that are widely discussed in Eastmond's review.[23] Furthermore, the fraction of carbonyl groups of PCL that hydrogen bonded with hydroxyl groups of a hydrogen bond donating polymer can be calculated by FTIR analysis. This technique allows the interassociation equilibrium constant (K_A) between hydroxyl groups of hydrogen bond donating polymers and carbonyl groups of PCL to be calculated at different temperatures and compositions by using the Painter−Coleman association model (PCAM).[24] However, this technique cannot be used directly to determine, by IR analysis, the interassociation equilibrium constant between the hydrogen bond donating hydroxyl groups and the PEO ether units in such binary blends because no carbonyl group is available to calculate the fraction of the hydrogen bonded ether group. The ether stretching mode near 1100−1200 cm^{-1} is a highly coupled mode that is conformationally sensitive and cannot be readily resolved into two peaks with areas corresponding to the free and the hydrogen-bonded ether absorptions.[25]

For convenience, we chose to study the different hydrogen bonging strengths in PCL blends with three different well-known hydrogen bond donating polymers: phenolic, PVPh, and phenoxy. Cortazar et al. studied the crystallization kinetics and melting behavior of the phenoxy/PCL blend and found that the surface free energy of chain folding of the PCL blend with phenoxy is lower than that of the pure PCL.[26] The same trend of surface free energy of chain folding was also observed in poly(vinyl chloride) (PVC)/PCL[23] and poly(styrene-*co*-acrylonitrile) (SAN)/PCL[27] blend systems. In our previous study of the phenolic/PCL blend system,[28] however, we found that the surface free energy of chain folding increases with increasing phenolic content. According to the secondary nucleation theory,[1,29] the initial crystal thickness is not only dependent on the degree of supercooling but also dependent on the value of the surface free energy of chain folding. As a result, determining the surface free energy of chain folding is quite important because the morphology of a crystalline PCL blend depends strongly on this value. The hydrogen bonding interaction that exists in phenoxy/PCL and phenolic/PCL blends has been discussed widely, but two different trends on the surface free energy of chain folding have been found. These trends indicate that different hydrogen bonding strengths can induce different polymer crystallization behaviors with respect to thermodynamic properties and morphologies.

According to the PCAM, the equilibrium constants for hydrogen bonding by self-association (K_B) and interassociation (K_A) can be obtained by Fourier transform infrared spectroscopy. Most importantly concerning the miscibility in this model is that if the interassociation is strongly favored over the self-association, the polymer blend is expected to be miscible. Conversely, if the self-association is stronger than the interassociation, the blend tends to be immiscible or partially miscible. As a result, two different types of hydrogen bonding strengths have been observed based on the PCAM. In this paper, we report the crystallization kinetics, surface free energies of chain folding, and crystalline thickness in PCL blends with phenolic, PVPh, and phenoxy, which we have studied by differential scanning calorimetry, Fourier transform infrared spectroscopy, optical microscopy, and small-angle X-ray scattering based on the PCAM. Good correlations exist, based on the PCAM, between the values of the surface free energies of chain folding and the relative ratio (K_A/K_B) of the inter- and self-association equilibrium constants.

Experimental Section

Materials. The PCL used in this study was the TONE Polymer P-787 with $M_n = 80\,000$ g/mol, which was purchased from Union Carbide Corp. The phenolic was synthesized with sulfuric acid via a condensation reaction, and average molecular weights are $M_n = 500$ g/mol and $M_w = 1200$ g/mol. The poly(vinylphenol) with a $M_w = 9000-10000$ g/mol were purchased from Polyscience Inc. The phenoxy was obtained from the Union Carbide Co., with $M_n = 23\,000$ g/mol and $M_w = 48\,000$ g/mol.

Blend Preparation. Blends of phenolic/PCL, PVPh/PCL, and phenoxy/PCL of various compositions were prepared by solution blending. Tetrahydrofuran solution containing 5 wt % of the polymer mixture was stirred for 6−8 h, and then the solvent was evaporated slowly at room temperature for 1 day. To ensure total elimination of solvent, the film of the blend was then dried at 50 °C for 2 days.

Characterizations. The crystallization behavior of the polymer blends was studied by DSC using a Du-Pont (DSC-9000). DSC was used to study the isothermal crystallization from the melt at 80 °C for 10 min, cooled rapidly to crystallization temperature (T_c), and then maintained at T_c for 12 h. In the crystallization experiments, crystallinity was expressed as the ratio of peak areas at time to that at the end of crystallization.

Infrared spectra of polymer blend films were determined by using the conventional NaCl disk method. The THF solution containing the blend was cast onto a NaCl disk and dried under condition similar to that used in the bulk preparation. The film used in this study was thin enough to obey the Beer−Lambert law. FTIR measurement was recorded on a Nicolet Avatar 320 FT-IR spectrophotometer, and 32 scans were collected with a spectral resolution of 1 cm^{-1}. IR spectra recorded at elevated temperatures were obtained by using a cell mounted inside the temperature-controlled compartment of the spectrometer.

The spherulite growth rates were determined by using a polarized-light microscope, manufactured by Olympus Limited Co., Japan, equipped with a heating stage (Mettler- FP90) and photographed with a CCD camera. Each sample was sandwiched between two thin glass slides, melted for 10 min on one hot stage at 80 °C, and then transferred as quickly as possible onto another hot stage preheated to the desired crystallization temperature (T_c). The samples were crystallized isothermally at a given T_c to monitor the growth of the spherulite as a function of time. The radial growth rate of a PCL spherulite was calculated as the slope of the line obtained from a plot of the spherulitic radius vs time.

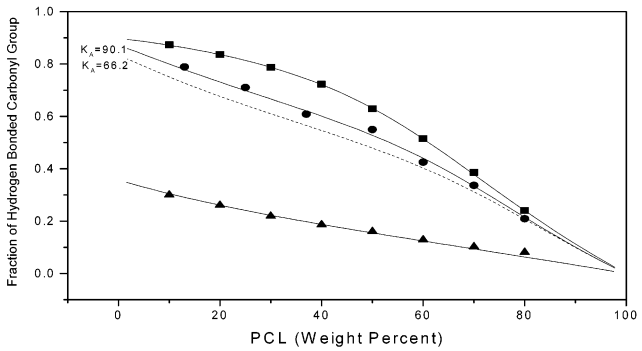

Figure 1. Relationship between experimental data and theoretical prediction by PCAM of hydrogen bonded fraction of carbonyl group within various PCL blend systems: (■) phenolic/PCL, (●) PVPh/PCL, (▲) phenoxy/PCL.

All SAXS measurements were performed at room temperature. The X-ray source was an 18 kW rotating-anode X-ray generator equipped with a rotating-anode Cu target. The X-ray source was operated at 200 mA and 40 kV.

Results and Discussion

Thermal Property and Hydrogen Bonding Strength in PCL Blend. In our previous study,[30] all PCL blends with phenolic, PVPh, and phenoxy exhibit a single glass transition temperature by DSC, which is a characteristic of miscible systems. The strength of interassociation, which was determined by calculating values of q in the Kwei equation,[31] depends on the hydrogen bonding donor group in the order phenolic/PCL > PVPh/PCL > phenoxy/PCL. In addition, the interaction energy density parameter calculated from the melting point depression of PCL using the Nishi−Wang equation[32] from the Flory−Huggins theory[33] also results in a similar trend as that of the Kwei equation.

Quantitative analyses of the fractions of hydrogen-bonded carbonyl groups in the molten state of all systems were made by FTIR spectroscopy. Figure 1 summarizes the fraction of hydrogen bonded carbonyl groups vs the PCL content for phenolic, PVPh, and phenoxy at 75 °C (above the melting temperature of PCL)[34] and indicates that the fraction of hydrogen bonded carbonyl groups increases with increasing content of these hydrogen bond donating polymers. Furthermore, it is clear that the fraction of hydrogen bond formation with PCL also occurs in the order phenolic/PCL > PVPh/PCL > phenoxy/PCL blend. In this study, we focus on their corresponding inter- and self-association equilibrium constants. In previous studies, values of K_B were calculated to be 52.3 for phenolic,[35] 66.8 for PVPh,[24] and 25.6 for phenoxy,[36] and values of dimer self-association equilibrium constant (K_2) were calculated to be 23.3, 21.0, and 14.4 for phenolic, PVPh, and phenoxy, respectively, at 25 °C. The values for the interassociation equilibrium constants of 116.83 and 7.0 for the phenolic/PCL and phenoxy/PCL blend system, respectively, have been calculated by us[34] and Iriarte et al.[37] Theoretical predictions agree with the values for the fraction of hydrogen bonded carbonyl group of the phenolic/PCL and phenoxy/PCL blends at 75 °C. However, in the present study, the experimental fraction of hydrogen bonded carbonyl groups in PVPh/PCL shows a larger deviation than that predicted using $K_A = 66.2$ in a previous study by Coleman et al.[38] Apparently, we have found that more suitable value of K_A is 90.1 for the PVPh/PCL blend based on the experimental data and theoretical prediction. Our calculation of the interassociation equilibrium constants followed a least-squares method that we have discussed previously.[39] Table 1 lists all the parameters required by the PCAM to estimate thermodynamic properties for these polymer blends. Clearly, the interassociation equilibrium constant and relative ratio of K_A/K_B occurs in the order phenolic/PCL > PVPh/PCL > phenoxy/PCL. Most importantly, we found that the value of K_A is greater than that of K_B in the phenolic/PCL and PVPh/PCL blend systems, while the reverse is true in the phenoxy/PCL blend system. These results indicate that in phenolic/PCL and PVPh/PCL blends the intermolecular hydrogen bonding dominates over the intramolecular hydrogen bonding for pure phenolic and pure PVPh homopolymers. In contrast, the intramolecular hydrogen bonding of the pure phenoxy homopolymer dominates over the intermolecular hydrogen bonding of the hydroxyl−carbonyl groups in the phenoxy/PCL blend system. The phenoxy/PCL blend has been defined in many previous studies as a strongly hydrogen bonding system.[26,39−44] Actually, our results suggest that the phenoxy/PCL blend is not really a strongly interacting system when compared with the phenolic/PCL and PVPh/PCL blends. Clearly, the interassociation strength depends on the nature of the hydrogen bond donor group and occurs in the order phenolic/PCL > PVPh/PCL > phenoxy/PCL based on the PCAM, and this order is consistent with previous DSC and FTIR analyses.

Isothermal Crystallization Kinetics. In this study of the isothermal crystallization by using DSC, the weight fraction of crystallinity, $X(t)$, was calculated according to the following equation:[45,46]

$$X(t) = \frac{\int_0^t \frac{dH}{dt}\,dt}{\int_0^\infty \frac{dH}{dt}\,dt} \qquad (1)$$

where the integral in the numerator is the heat generated at time t and that in the demominator is the total heat generated up to the end of the crystallization process. For brevity, Figure 2 shows the typical isotherms obtained by plotting $X(t)$ against time for pure PCL, phenolic/PCL, PVPh/PCL, and phenoxy/PCL with the same hydrogen bond donating polymer content (10 wt %) at the crystallization temperature of 40 °C. The crystallization kinetics of the PCL blends were analyzed using the Avrami treatment:[47]

$$\log[-\ln(1 - X_t)] = \log k + n \log(t) \qquad (2)$$

where $X(t)$ is the weight faction of material crystallized after time t, n is the Avrami exponent, the value of which depends both on nature of the primary nucleation and on the growth geometry of the crystalline entities, and k is the overall kinetic rate constant, which depends on the rates of nucleation and growth. The values of k and n can be calculated from the intercept and slope of eq 2. Figure 3 shows that a linear relationship exists between $\log[-\ln(1 - Xt)]$ and $\log t$ for pure PCL, phenolic/PCL, PVPh/PCL, and phenoxy/PCL with the same composition at the crystallization temperature of 40 °C. In addition, from Figure 2, the half-time of crystallization, $t_{1/2}$, is defined as the time required for half of the final crystallinity to be developed. Figure 4 displays a plot of $t_{1/2}$ vs T_c for phenolic/PCL, PVPh/PCL, and phenoxy/PCL blends. For the sake of brevity, the

Table 1. Summary of the Self- and Interassociation Equilibrium Constants and Their Thermodynamic Parameter of Phenolic/PCL, PVPh/PCL, and Phenoxy/PCL Blends at 25 °C[a]

					equilibrium constant			enthalpy (kcal/mol)		
polymer	V	M_w	δ	DP	K_2	K_B	K_A	h_2	h_B	h_A
phenolic[b,c]	84	105	12.05	6	23.3	52.3	116.8	−4.1	−6.1	−4.6
PVPh[d]	100	120	10.60	100	21.0	66.8	90.1	−5.6	−5.2	−4.3
phenoxy[e,f]	216	284	10.22	80	25.6	14.4	7.0	−2.5	−3.4	−2.7
PCL[d]	107	114	9.21	714						

[a] V = molar volume (mL/mol), M_w = molecular weight (g/mol), δ = solubility parameter (cal/mL)$^{1/2}$, DP = degree of polymerization, K_2 = dimer self-association equilibrium constant, K_B = multimer self-association equilibrium constant, K_A = interassociation equilibrium constant, h_2 = enthalpy of dimer self-association formation, h_B = enthalpy of multimer self-association formation, and h_A = enthalpy of interassociation formation. [b] Reference 35. [c] Reference 34. [d] Reference 24. [e] Reference 36. [f] Reference 37.

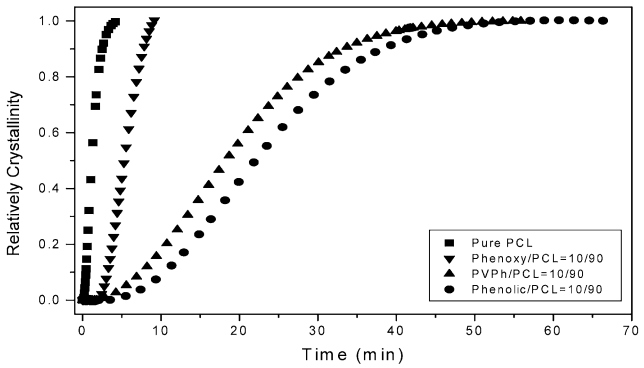

Figure 2. Crystallization isotherms of pure PCL, phenolic/PCL = 10/90, PVPh/PCL = 10/90, and phenoxy/PCL = 10/90 blends at 40 °C.

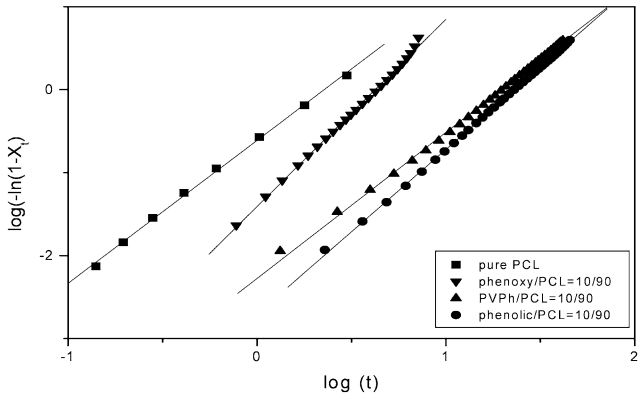

Figure 3. Avrami plot for pure PCL, phenolic/PCL = 10/90, PVPh/PCL = 10/90, and phenoxy/PCL = 10/90 blends at 40 °C.

values of k, n, and $t_{1/2}$ are not shown in this study. However, we found noninteger values of n in almost all cases resulting from mixed growth or surface nucleation modes. The values of k decrease with increasing the hydrogen bond donor content and the crystallization temperature. It is well-known that molecular mobility is the controlling factor at lower crystallization temperatures, while at higher crystallization temperatures the process is controlled by nucleation, such that k decreases with increasing T_c. Most importantly, these results also indicate that the overall crystallization rate decreases in the order phenolic/PCL > PVPh/PCL > phenoxy/PCL, which is also consistent with the order of increasing strength of hydrogen bonding.

Spherulite Growth Kinetics. The spherulite growth rates of PCL blends were determined by using a polarizing optical microscope. Figure 5 displays plots of the spherulite radius of pure PCL, phenolic/PCL, PVPh/PCL, and phenoxy/PCL vs time under same composition at the crystallization temperature of 40 °C. The solid lines represent the best least-squares fits to the data. It is clear that there is a linear increase in the radius with time until the spherulite impinges on one another, with the slopes of the lines increasing in the order pure PCL > phenoxy/PCL > PVPh/PCL > phenolic/PCL. The dependence of G on T_c for pure PCL and various PCL blends is shown in Figure 6, which indicates that the spherulite growth rate decreases with an increase in the content of the hydrogen bond donating polymer at a given value of T_c. The presence in the blends of amorphous hydrogen bond donating polymers with high values of T_g significantly decreases the rate of PCL crystallization, as is expected. Furthermore, the reduction in the spherulite growth rate also decreases with increasing the crystallization temperature. Similarly, these results also indicate that the spherulite growth rate decreases in the order phenolic/PCL > PVPh/PCL > phenoxy/PCL, which is also consistent with the order of hydrogen bonding strength. In general, there are three main factors dictating the depression of crystallization rate in the miscible crystalline/amorphous polymers with high T_g: (1) a decrease of segmental mobility of the crystalline polymer transporting across the liquid−solid interface because of the high T_g of the blends, (2) a dilution effect that reduces the number of crystallizable segments at the surface of the growth spherulite, and (3) a decrease in supercooling resulting from the depression in melting point.

Values of interaction energy density parameters, calculated from melting depression of PCL using the Nishi−Wang equation in our previous study,[30] follow the order phenolic/PCL > PVPh/PCL > phenoxy/PCL, which implies that the degree of supercooling is inversely proportional to the hydrogen bonding strength at a constant crystallization temperature. Therefore, the crystallization rate depression in the present study is consistent with the degree of supercooling. Nonetheless, in a previous study, Wang and Jiang[48] found that the dependence of the decrease in the crystallization growth rate on glass transition temperature in the SAN/PCL blend dominates over the polymer−polymer interaction parameter based on the Flory−Huggins theory. The glass transition temperatures of phenolic, PVPh, and phenoxy are 66, 150, and 98 °C, respectively, and the T_g order is PVPh > phenoxy > phenolic. Apparently, the glass transition temperature does not play the main role in determining the crystallization kinetics in a blend system with strong hydrogen bonding interactions. It seems that the hydrogen bonding strength or the polymer−polymer interaction parameter is more important than the chain mobility in a hydrogen-bonded PCL blend system. On the contrary, the influence of the glass transition temperature of the blend, which is related to the chain mobility, is more important than

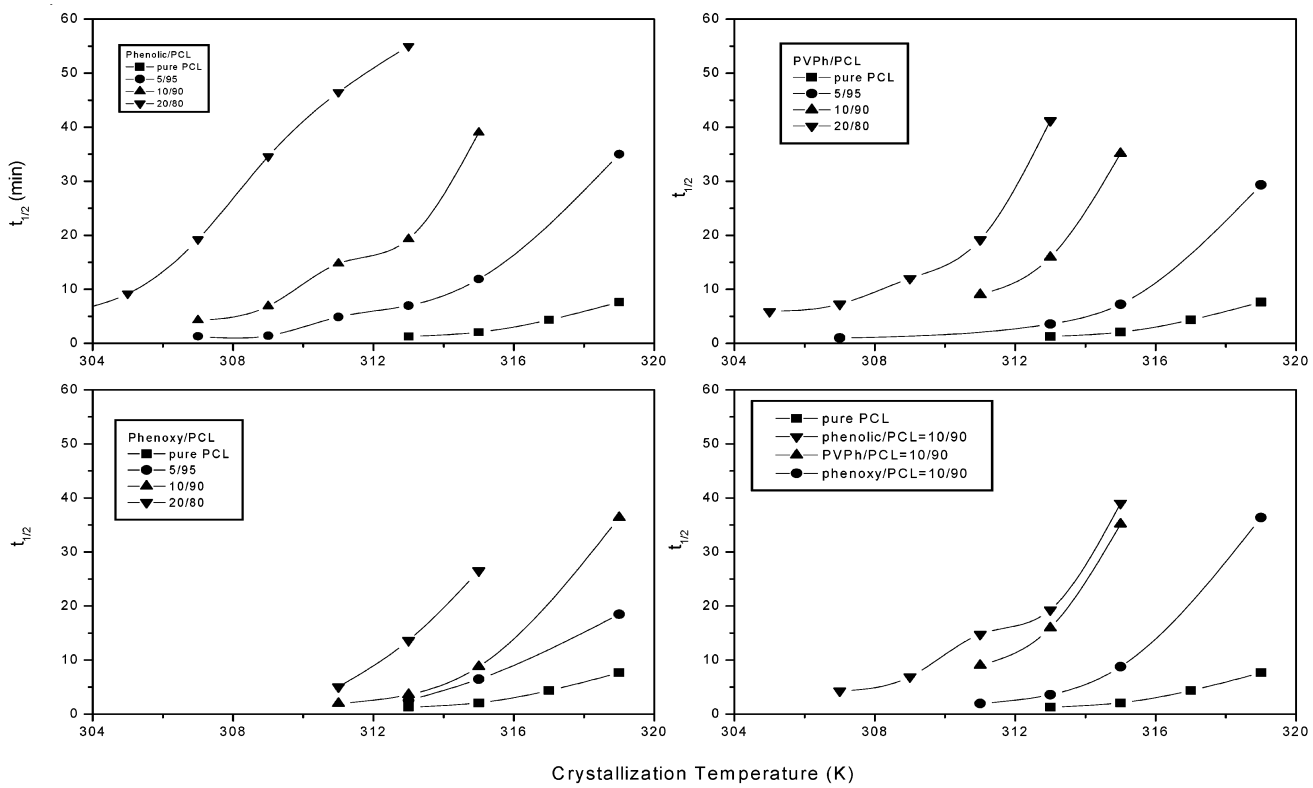

Figure 4. Plot of $t_{1/2}$ vs crystallization temperature for samples of different compositions of phenolic/PCL, PVPh/PCL, and phenoxy/PCL blends.

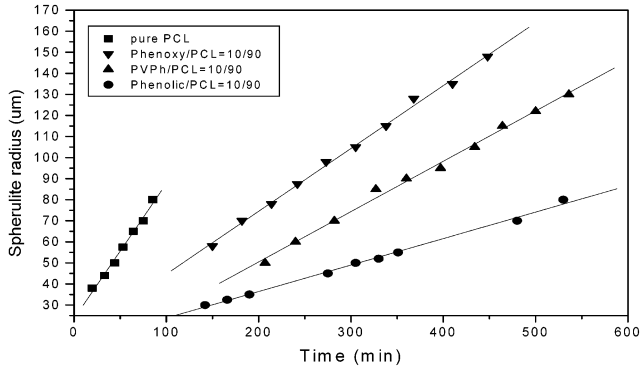

Figure 5. Spherulite radius as a function of time for pure PCL, phenolic/PCL = 10/90, PVPh/PCL = 10/90, and phenoxy/PCL = 10/90 blends isothermally crystallized at 40 °C.

the polymer−polymer interaction parameter in a blend system with relatively weak interactions.

The Lauritzen−Hoffman model, described below, was used to analyze the spherulite crystallization behavior of homopolymers and some crystalline/amorphous polymer blends. We have also used this theory to analyze the spherulite crystallization behavior of PCL blends. The equation is[49]

$$G = G_0 \exp\left[\frac{-U^*}{R(T - T_\infty)}\right] \exp\left[\frac{-K_g}{f\,T\Delta T}\right] \qquad (3)$$

where G_0 is the front factor, U^* is the activation energy for the segment diffusion to the site of crystallization, R is the gas constant, T_∞ is the hypothetical temperature below which all viscous flow ceases, K_g is the nucleation parameter, ΔT is the degree of supercooling defined by $T_m^0 - T_c$, and f is a correction factor given as $2T_c/(T_m^0 + T_c)$. It is important to emphasize that the parameters U^* and T_∞ were treated as variables to maximize the quality of the fit to eq 3. In this study, we used the Williams−Landel−Ferry (WLF) values of $U^* = 4120$ cal/mol and $T_\infty = T_g - 51.6$.[50] The nucleation parameter K_g is given by[51,52]

$$K_g = \frac{nb\sigma\sigma_e T_m^0}{\Delta h_f k_B} \qquad (4)$$

where b is the thickness of a monomolecular layer, σ is the lateral surface free energy, σ_e is the surface free energy of chain folding, Δh_f is the heat of fusion per unit volume, T_m^0 is the equilibrium melting temperature, and k_B is the Boltzmann constant. Typically, the value of $n = 4$ in regimes I and III, but a value of $n = 2$ was employed in regime II. Often, it is most convenient to rearrange eq 3 as

$$\ln G + \frac{U^*}{R(T - T_\infty)} = \ln G_0 - \frac{K_g}{T(\Delta T)f} \qquad (5)$$

A plot of the left-hand side of eq 5 vs $1/T_c(\Delta T)f$ gives a line of slope $= -K_g$. The values of K_g from eq 5 analyses are summarized in Table 2. In this study, the regime is assigned to be regime II at 30−40 °C.[26] The derived value of K_g can be used to calculated σ_e and the work of chain folding q for the PCL. Using the thickness $b = 0.412$ nm,[52] $T_m^0 = 70.9$ °C was determined in our previous study[34] and $\Delta h_f = 1.63 \times 10^9$ erg/cm^3.[53] The lateral surface free energy σ may be estimated by the Thomas−Stavely relationship:[54]

$$\sigma = \alpha b_0 (\Delta h_f) \qquad (6)$$

where α is an empirical constant and α is usually assumed to be 0.1 for the vinyl polymers and $\alpha = 0.25$

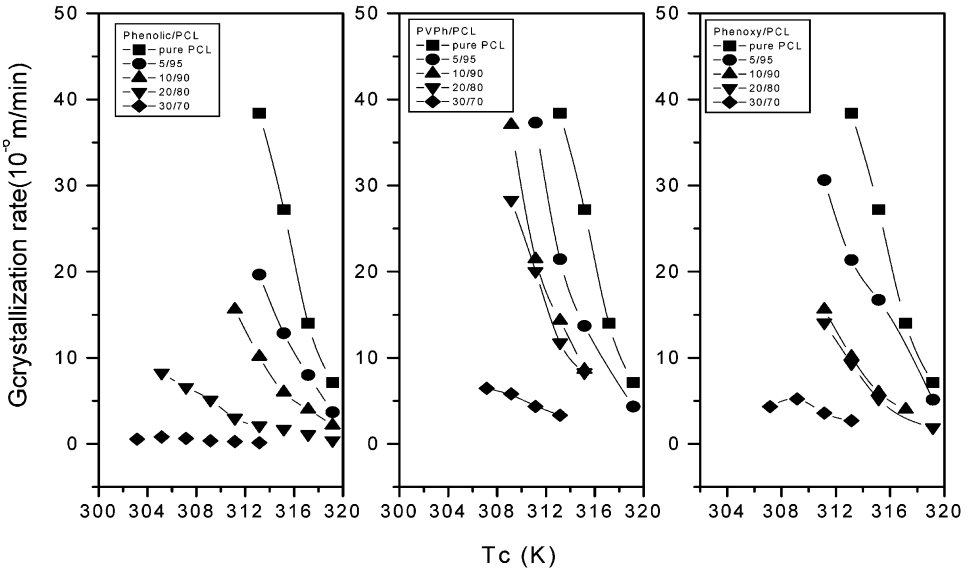

Figure 6. Radial growth rate (G) as a function of T_c for phenolic/PCL, PVPh/PCL, and phenoxy/PCL blends.

Table 2. Comparison of K_g and Surface Free Energies of Chain Folding for Phenolic/PCL, PVPh/PCL, and Phenoxy/PCL Blends

compositions	K_g(II) × 10^{-4} (deg^2)	σ_e (erg/cm^2)
phenolic/PCL		
0/100	9.90	72.36
5/95	10.0	72.68
10/90	10.4	75.48
20/80	12.2	88.96
30/70	13.3	96.56
PVPh/PCL		
0/100	9.90	72.36
5/95	10.3	74.68
10/90	11.3	82.12
20/80	11.5	83.58
30/70	11.8	85.76
phenoxy/PCL		
0/100	9.90	72.36
5/95	8.95	65.04
10/90	9.60	69.77
20/80	9.65	70.13
30/70	9.70	70.49

for high melting polyesters.[55] For a low-melting polyester, such as PCL, which has a long sequence of CH_2 groups as in PE, a value of 0.1 is recommended. The value of σ_e for pure PCL was obtained as 72.36 erg/cm^2, which agrees well with the value previously reported.[26] The values of K_g(II) and σ_e with respect to blend compositions are also listed in Table 2. Both values increase with the increase in the content of phenolic and PVPh, indicating that the crystallization ability of PCL decreases with increasing content of phenolic and PVPh in blends. However, the surface free energy of chain folding decreases with an increase in phenoxy content up to phenoxy/PCL = 5/95 and then increases with increase of phenoxy content. We emphasize here that the surface free energy of chain folding in phenoxy/PCL is still lower than that of the pure PCL. It seems that the value of surface free energy of chain folding is dependent on the relative ratio of K_A to K_B based on the PCAM. To confirm this assumption, Table 3 lists various hydrogen bonded crystalline polymer blends in which the relative strength of K_A/K_B and their corresponding values of surface free energy of chain folding have been studied. Clearly, if the K_A is larger than the K_B, the value of surface free energy in the polymer blend is larger than that in the pure crystalline homopolymer, as in the case for the phenolic/PCL, PVPh/PCL, and phenolic/PEO[56] blend systems. Conversely, if the K_B is greater than the K_A, the value of surface free energy in the polymer blend is smaller than that in the pure crystalline homopolymer, as in the cases of the phenoxy/PCL[26] and PVPh/PHB[57] blend systems. In addition, the value of surface free energy in a polymer blend with a relatively weaker interaction is smaller than that in the pure crystalline homopolymer, as in the case for PVC/PCL,[23] SAN/PCL,[27] and PMA/PHB.[58]

Although the crystallization kinetics rate was observed to decrease with an increase in the amount of the amorphous component in all these miscible blend systems, the values of surface free energy of chain folding show different trends with different intermolecular interaction strengths. In a blend system with strong hydrogen bonding, the value of surface free energy of chain folding increases with an increase in the content of phenolic or PVPh. These results are probably related to the fact that during crystallization phenolic and PVPh may easily form entanglements or physical cross-links with PCL molecules, which favors the formation of large loops on the surface of PCL lamellar crystals.[59] This result indicates that the surface enthalpy term overwhelms the surface entropy of chain folding because of the fact that K_A is greater than K_B. On the contrary, in a blend system with weak hydrogen bonding, the phenoxy may act as a nucleation agent for PCL since K_B is greater than K_A; the blend tends to be immiscible or partially miscible and thus reduce the free energy change on crystallization and the driving force for crystallization. The same explanation has been used in a relative weakly interacting blend, such as the SAN/PCL blend.[27] A recent theoretical model has predicted that a miscible blend of polymers with a relatively large T_g difference, and that exhibit weak intermolecular interactions, will exhibit "two dynamic microenvironments".[60] One is near the mean blend mobility, and the other is close to that of the component with lower T_g. Even though the weakly hydrogen bonding blends, such as phenoxy/PCL, and the weakly interacting blends, such as PVC/PCL or SAN/PCL blend systems, show only one single T_g based on DSC analyses. It is generally known that a single compositionally dependent T_g indicates full miscibility with a dimension on the order

Table 3. Relationship between the Relative Magnitude Strength of K_A vs K_B with Surface Free Energy of Chain Folding and Crystal Layer Thickness

blend system	K_A	K_B	relative magnitude strength of K_A vs K_B	σ_e compared with pure crystallizable component	l_c compared with pure crystallizable component
			Strongly Hydrogen Bonding		
phenolic/PCL	116.8[a]	52.3[b]	$K_A > K_B$	increase[c]	increase[c]
PVPh/PCL	90.1[d]	66.8[e]	$K_A > K_B$	increase[d]	increase[d,f]
phenolic/PEO	264.7[g]	52.3[b]	$K_A > K_B$	increase[h]	—[ac]
SHS50/PEO	39.3[i]	29.8[e]	$K_A > K_B$	—[ac]	increase[j]
			Weakly Hydrogen Bonding		
phenoxy/PCL	7.0[k]	25.6[l]	$K_A < K_B$	decrease[d,m]	decrease[d,n]
PVPh/PLLA	10[o]	66.8[e]	$K_A < K_B$	—[ac]	decrease[p]
PVPh/PHB	62.1[q]	66.8[e]	$K_A < K_B$	decrease[r]	decrease[r]
ACA/PHB	2.6[ab]	28.8[ab]	$K_A < K_B$	decrease[s]	decrease[s]
			Weakly Interaction		
PVC/PCL				decrease[t]	decrease[u]
SAN/PCL				decrease[v]	decrease[x]
PMA/PHB				decrease[y]	—[ac]
PVAc/PHB				—[ac]	increase[z]
PVAc/PEO				—[ac]	increase[aa]

[a] Reference 34. [b] Reference 35. [c] Reference 28. [d] This study. [e] Reference 24. [f] Reference 67. [g] Reference 75. [h] Reference 56. [i] Reference 24. [j] Reference 21. [k] Reference 37. [l] Reference 36. [m] Reference 26. [n] Reference 39. [o] Reference 76. [p] Reference 74. [q] Reference 73. [r] Reference 57. [s] Reference 22. [t] Reference 23. [u] Reference 68. [v] Reference 27. [x] Reference 66. [y] Reference 58. [z] Reference 71. [aa] Reference 72. [ab] Reference 77; the K_B of ACA is used the K_B of ethylene-*co*-vinyl alcohol (EVOH), and the K_A between ACA and PHB is used the K_A between EVOH and PVAc. [ac] Some unknown results are not shown in this table based on our knowledge.

of 20−40 nm, but it does not confirm the fully miscible domain size below this dimension. For example, the well-known hydrogen bonded blend system PVPh/PMMA has been observed to exhibit only one single value of T_g based on DSC analyses.[61] However, two dynamic relaxations are found by using a dynamic mechanical analyzer and observing the spin−lattice relaxation time in the rotating frame ($T_{1\rho}$(H)) in solid-state nuclear magnetic resonance spectroscopy[62−64] since the value of K_A between the hydroxyl group of PVPh and the carbonyl group of PMMA ($K_A = 37.5$) is smaller than the value of K_B for the hydroxyl−hydroxyl interactions of PVPh ($K_B = 66.8$).[61] Two relaxation times in the rotating frame indicate that the immiscibility domain size is greater than 2−3 nm based on the one-dimensional spin-diffusion equation. Therefore, microphase separation may occur in certain relative weakly hydrogen bonding or weakly interacting blend system, indicating that the amorphous component may play the role of a nucleation agent to reduce the surface free energy of chain folding and provide the driving force for crystallization.

Morphology. Small-angle X-ray scattering is a powerful tool for probing the detailed microstructure of crystalline/amorphous blends. The morphological parameters in the lamellar level, such as the long period (L), crystal layer thickness (l_c), and amorphous layer thickness (l_a), can be determined from the one-dimensional correlation function.[65] Figure 9 shows the profiles of Lorentz-corrected intensity (Iq^2) of pure PCL, phenolic/PCL, PVPh/PCL, and phenoxy/PCL with the same compositions at the crystallization temperature of 40 °C for 1 week. The peak position shifts toward a lower angle with increasing the content of all the hydrogen-bond donating polymers, indicating that the long period from Bragg's law increases. This phenomenon may result from the thickness of the PCL crystals or the swelling of amorphous layers by blending with the hydrogen bond donor polymers. This kind of increase in the lamellar periodicity of a crystallizable component in a polymer blend attributable to interlamellar segregation of the second amorphous component has been observed for the SAN/PCL,[66] PVPh/PCL,[67] and PHB/PVPh[57] blend systems. This result indicates that during

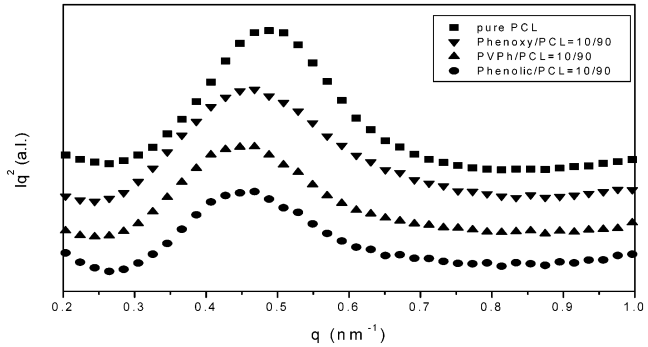

Figure 7. Profiles of Lorentz-corrected SAXS intensity of phenolic/PCL blends pure PCL, phenolic/PCL = 10/90, PVPh/PCL = 10/90, and phenoxy/PCL = 10/90 blends isothermally crystallized at 40 °C for 1 week.

crystallization of PCL from the one-phase melt the amorphous hydrogen bond donating polymer is rejected into the interlamellar region of PCL, where it forms a homogeneous blend with the amorphous region of PCL molecules.

For convenience, the crystal layer thickness of PCL blends in this study are adapted from previous studies by us,[28] Chen et al.,[67] and Defieuw.[39] We have found that the crystal layer thickness of PCL increases with an increase in the phenolic and PVPh content. The same trend of increasing crystal layer thickness was also found in the poly(styrene-*co*-vinylphenol)/PEO blend system.[21] In contrast, the crystal layer thickness of the phenoxy/PCL blend is almost lower than that of pure PCL reported previously by Defieuw et al.[39] The crystal layer thickness of PCL varied with the phenoxy content and exhibited a maximum at 20 wt % of phenoxy. In other blend compositions, the crystal layer thickness of PCL is less than that in pure PCL. The same reduction of crystal thickness has also been found in weakly interaction blend such as PVC/PCL[68] and SAN/PCL.[69]

According to the secondary nucleation theory, the initial crystal thickness is given by[1,29]

$$l_g^* \cong \frac{2\sigma_e T_m^0}{\Delta h_f^0 (T_m^0 - T_c)} \tag{7}$$

The final crystal thickness, according to the notation of Hoffman and Weeks,[70] is γ times the initial thickness:

$$l_c = \gamma l_g^* \tag{8}$$

where γ is the lamellar thickness factor. In general, the formation of thicker crystals in the blend is attributed to the depression of the equilibrium melting temperature because the initial crystal thickness is inversely proportional to the degree of supercooling in eq 7. Depression of the equilibrium melting temperature by blending lowers the degree of supercooling for a given T_c and a large l_g^* is induced in the blend. It is well-known that a depression of equilibrium melting temperature is found in most miscible systems, which reduces the formation of thicker crystals. However, as mentioned above, the reduction of crystal thickness has been found, as in the cases of PVC/PCL and SAN/PCL. Apparently, it is clear that the initial crystal thickness is not only dependent on degree of supercooling but is also dependent on the values of the surface free energy of chain folding in eq 7. The initial crystal thickness is proportional to the surface free energy of chain folding in eq 7. As a result, the crystal layer thickness depends on the competition between the values of surface free energy of chain folding and the degree of supercooling. Table 3 also lists different values of the surface free energy of chain folding and the crystal layer thickness compared with those of the pure crystallizable component, in various crystalline/amorphous blends. When the uncomplicated blend system is strongly hydrogen bonding, as in the cases of the phenolic/PCL and PVPh/PCL blend systems, the surface free energy of chain folding is larger than that of pure PCL and the degree of supercooling is lower than that of pure PCL, which suggests that the crystal layer thickness of PCL is increased with increasing the phenolic and PVPh content. However, the crystal layer thickness of phenoxy/PCL has a lower value than that of pure PCL since the surface free energy of chain folding is lower than that of pure PCL. In another previous study,[26] Cortazar et al. found that the surface free energy of chain folding of phenoxy/PCL is also lower than the pure PCL with the all compositions of phenoxy content. Therefore, the competition between the lower value of the surface free energy of chain folding and the lower degree of supercooling, relative to those of pure PCL, induces the smaller crystal layer thickness. Meanwhile, a reduction of the surface free energy of chain folding was found in weakly interacting systems, such as PVC/PCL and SAN/PCL blends, in which the thickness of the crystalline phase decreases with an increase in the PVC and SAN content. This phenomenon may arise from the surface free energy of chain folding dominating over the degree of supercooling. In contrast, for the same weakly interacting blend system of PVAc/PHB[71] and PVAc/PEO,[72] blending with PVAc results in thickening of the PHB and PEO crystals. This phenomenon can be interpreted by considering that the degree of supercooling is predominant. We have confirmed that the thickness of a crystalline phase is also strongly dependent on the value of the surface free energy of chain folding. Here, an interesting question arises: Can we establish a general principle for predicting the thickness of crystalline phase in a miscible polymer blend?

Interestingly, we note with that if the interassociation equilibrium constant is greater than the self-association equilibrium constant in a blend system exhibiting strong hydrogen bonding, the crystal layer is expected to be relatively thicker, as in the cases of phenolic/PCL, PVPh/PCL, and SHS50/PEO, because of the larger surface free energy of chain folding and/or the lower degree of supercooling. The general reduction in crystal layer thickness is expected in blend systems displaying weak hydrogen bonding, such as phenoxy/PCL, PVPh/PHB,[22,57] PVPh/PLLA,[73] and ACA/PHB,[74] because the lower surface free energy is predominant over the lower degree of supercooling. The most complicated blend systems are those with weakly interacting components, such as PVC/PCL, SAN/PCL, PVAc/PEO, and PVAc/PHB, and they exhibit either increases or decreases in crystal layer thickness. This phenomenon is dependent on whether the lower surface free energy of chain folding or the lower degree of supercooling is predominant.

In summary, the microstructure, morphology, and crystallization kinetics of crystalline/amorphous binary blends are quite complicated. There are several main factors that influence their behavior, including the glass transition temperature that is related to the chain mobility,[48] specific interactions such as hydrogen bonding, dipole−dipole interactions, or copolymer repulsive effects, polymer−polymer interaction parameter that is related to the degree of supercooling, and molecular weight.[68] In this paper, we have demonstrated that different hydrogen bonding strengths may lead to different thermodynamic, morphologic, and kinetic properties. In a blend system exhibiting strong hydrogen bonding, the strength of the intermolecular interaction plays the most important role relative to others factor. By strong or weak hydrogen bonding, we refer to the relative magnitude of the interassociation and self-association equilibrium constants.

Conclusions

The reduced overall crystallization kinetics and crystal growth rate in PCL crystalline phases are in the order phenolic/PCL > PVPh/PCL > phenoxy/PCL, which is consistent with their relative intermolecular hydrogen bonding strengths based on the Painter−Coleman association model. This result suggests that the effect of hydrogen bonding strength on the rate of crystallization predominates over the influence of the glass transition temperature of the blends. The definition of strong or weak hydrogen bonding refers to the relative magnitudes of the interassociation and self-association equilibrium constants. The values of the surface free energy of chain folding in PCL crystalline phases is increased with increasing content of hydrogen bond donating polymer in the phenolic/PCL and PVPh/PCL blends, since the K_A of the hydroxyl−carbonyl interaction is greater than the K_B of the hydroxyl−hydroxyl interaction in these two blend systems. In contrast, in the phenoxy/PCL blend system, the smaller K_A relative to the K_B induces a smaller surface free energy of chain folding than that of the pure PCL. Different values of surface free energy of chain folding tend to induce different crystal layer thickness since this value is dependent on the competition between the values of surface free energy of chain folding and the degree of supercooling.

Acknowledgment. The authors thank the National Science Council, Taiwan, Republic of China, for financially supporting this research under Contract NSC-91-2216-E-009-018. We are also grateful to Prof. Tsang-

Lang Lin of the Department of Engineering and System Science at National Tsing Hua University for assistance in SAXS measurements.

References and Notes

(1) Hoffman, J. D.; Miller, R. L. *Polymer* **1997**, *38*, 3151.
(2) Flory, P. J. *J. Chem. Phys.* **1949**, *17*, 223.
(3) Flory, P. J. *J. Am. Chem. Soc.* **1962**, *84*, 2857.
(4) Mandelkern, L.; Alamo, R. G.; Kennedy, M. A. *Macromolecules* **1990**, *23*, 4721.
(5) Point, J. J.; Dosiere, M. *Macromolecules* **1989**, *22*, 3502.
(6) Russell, T. P.; Ito, H.; Wignall, G. D. *Macromolecules* **1988**, *21*, 1703.
(7) Defieuw, G.; Groeninckx, G.; Reynaers, H. *Polymer* **1989**, *30*, 595.
(8) Stein, R. S.; Khambatta, F. B.; Warner, F. P.; Russell, T. P.; Escala, A.; Balizer, E. *J. Polym. Sci., Polym. Symp.* **1978**, *63*, 313.
(9) Talibuddin, S.; Runt, J.; Liu, L. Z.; Chu, B. *Macromolecules* **1998**, *31*, 1627.
(10) Penning, J. P.; Manley, R. S. J. *Macromolecules* **1996**, *29*, 77.
(11) Russell, T. P.; Stein, R. S. *J. Polym. Sci., Polym. Phys. Ed.* **1982**, *20*, 1593.
(12) Russell, T. P.; Stein, R. S. *J. Polym. Sci., Polym. Phys. Ed.* **1983**, *21*, 999.
(13) Eersels, K. L.; Groeninckx, G.; Koch, M. H. J.; Reynaer, H. *Polymer* **1988**, *29*, 3893.
(14) Huo, P. P.; Cebe, P.; Capel, M. *Macromolecules* **1993**, *26*, 4275.
(15) Sauer, B. B.; Hsiao, B. S. *J. Polym. Sci., Polym. Phys. Ed.* **1993**, *31*, 901.
(16) Cheung, Y. W.; Stein, R. S.; Lin, J. S.; Wignall, G. D. *Macromolecules* **1994**, *27*, 2520.
(17) Saito, H.; Stuehn, B. *Macromolecules* **1994**, *27*, 216.
(18) Sadoco, P.; Canetti, M.; Seves, A.; Martuscelli, E. *Polymer* **1993**, *34*, 3368.
(19) Liu, L. Z.; Chu, B.; Penning, J. P.; Manley, R. S. J. *Macromolecules* **1997**, *30*, 4398.
(20) Keith, H. D.; Padden, F. J. *J. Appl. Phys.* **1975**, *35*, 1270.
(21) Talibuddin, S.; Wu, L.; Runt, J.; Lin, J. S. *Macromolecules* **1996**, *29*, 7527.
(22) Xing, P.; Ai, X.; Dong, L.; Feng, Z. *Macromolecules* **1998**, *31*, 6898.
(23) Eastmond, G. C. *Adv. Polym. Sci.* **1999**, *149*, 223.
(24) Coleman, M. M.; Graf, J. F.; Painter, P. C. *Specific Interactions and the Miscibility of Polymer Blends*; Technomic Publishing: Lancaster, PA, 1991.
(25) Menestrel, C. L.; Bhagwagar, D. E.; Painter, P. C.; Coleman, M. M.; Graf, J. F. *Macromolecules* **1992**, *25*, 7101.
(26) Juana, D. R.; Cortazar, M. *Macromolecules* **1993**, *26*, 1170.
(27) Li, W.; Yan, R.; Jing, X.; Jiang, B. *J. Macromol. Sci., Phys.* **1992**, *B31*, 227.
(28) Kuo, S. W.; Chan, S. C.; Chang, F. C. *J. Polym. Sci., Polym. Phys. Ed.*, in press.
(29) Hoffman, J. D.; Weeks, J. J. *J. Res. Natl. Bur. Stand. A: Phys. Chem.* **1962**, *66A*, 13.
(30) Kuo, S. W.; Huang, C. F.; Chang, F. C. *J. Polym. Sci., Polym. Phys. Ed.* **2001**, *39*, 1348.
(31) Kwei, T. K. *J. Polym. Sci., Polym. Lett. Ed.* **1984**, *22*, 307.
(32) Nishi, T.; Wang, T. T. *Macromolecules* **1975**, *8*, 909.
(33) Flory, P. J. *Principles of Polymer Chemistry*; Cornell University Press: Ithaca, NY, 1953.
(34) Kuo, S. W.; Chang, F. C. *Macromol. Chem. Phys.* **2001**, *201*, 3112.
(35) Wu, H. D.; Chu, P. P.; Ma, C. C. M.; Chang, F. C. *Macromolecules* **1999**, *32*, 3097.
(36) Espi, E.; Iruin, J. J. *Macromolecules* **1991**, *24*, 6456.
(37) Iriarte, M.; Alberdi, M.; Shenoy, S. L.; Iruin, J. J. *Macromolecules* **1999**, *32*, 2661.
(38) Coleman, M. M.; Lichkus, A. M.; Painter, P. C. *Macromolecules* **1989**, *22*, 586.
(39) Defieuw, G.; Groenincx, G.; Reynaers, H. *Polymer* **1989**, *30*, 2164.
(40) Vanneste, M.; Groenincx, G.; Reynaers, H. *Polymer* **1997**, *38*, 4407.
(41) Harris, J. E.; Goh, S. H.; Paul, D. R.; Barlow, J. W. *J. Appl. Polym. Sci.* **1982**, *27*, 839.
(42) Coleman, M. M.; Moskala, E. J. *Polymer* **1983**, *24*, 251.
(43) Juana, D. R.; Hernandez, R.; Pena, J. J.; Santamaria, A.; Cortazar, M. *Macromolecules* **1994**, *27*, 6980.
(44) Juana, D. R.; Jauregui, A.; Calahorra, E.; Cortazar, M. *Polymer* **1996**, *37*, 3339.
(45) Mancarella, C.; Martucelli, E. *Polymer* **1977**, *13*, 407.
(46) Wunderlich, B. *Macromolecular Physics*; Academic Press: New York, 1976.
(47) Avrami, M. *J. Chem. Phys.* **1939**, *7*, 1103.
(48) Wang, Z.; Jiang, B. *Macromolecules* **1997**, *30*, 6223.
(49) Hoffman, J. D.; Davis, G. T.; Lauritzen, J. I., Jr. In *Treatise on Solid State Chemistry*; Hannay, N. B., Ed.; Plenum Press: New York, 1976; Vol. 3.
(50) Williams, M. L.; Landel, R. F.; Ferry, J. D. *J. Am. Chem. Soc.* **1975**, *77*, 3701.
(51) Hoffman, J. D. *Polymer* **1983**, *24*, 3.
(52) Phillips, P. J.; Rensch, G. J.; Taylor, K. D. *J. Polym. Sci., Polym. Phys. Ed.* **1987**, *25*, 1725.
(53) Crescenzi, V.; Manzini, G.; Calzolari, G.; Borri, C. *Eur. Polym. J.* **1972**, *8*, 449.
(54) Thomas, D. G.; Staveley, L. A. K. *J. Chem. Soc.* **1952**, 4569.
(55) Rotiman, D. B.; Marand, H.; Miller, R. L.; Hoffman, J. D. *J. Phys. Chem.* **1989**, *93*, 6919.
(56) Zhong, Z.; Guo, Q. *Polymer* **2000**, *41*, 1711.
(57) Xing, P.; Dong, L.; An, Y.; Feng, Z.; Avella, M.; Martuscelli, E. *Macromolecules* **1997**, *30*, 2726.
(58) An, Y.; Dong, L.; Li, G.; Mo, Z.; Feng, Z. *J. Polym. Sci., Polym. Phys. Ed.* **2000**, *38*, 1860.
(59) Zhong, Z.; Guo, Q. *J. Polym. Sci., Polym. Phys. Ed.* **1999**, *37*, 2726.
(60) Kumar, S. K.; Colby, R. H.; Anastasiadis, H.; Fytas, G. *J. Chem. Phys.* **1996**, *105*, 3777.
(61) Serman, C. J.; Painter, P. C.; Coleman, M. M. *Polymer* **1991**, *32*, 1049.
(62) Zhang, X.; Takegoshi, K.; Hikichi, K. *Macromolecules* **1991**, *24*, 5756.
(63) Li, D.; Brisson, J. *Macromolecules* **1996**, *29*, 868.
(64) Dong, J.; Ozaki, Y. *Macromolecules* **1997**, *30*, 286.
(65) Strobl, G. R.; Schneider, M. *J. Polym. Sci., Polym. Phys. Ed.* **1980**, *18*, 1343.
(66) Li, W.; Yan, R.; Jiang, B. *Polymer* **1992**, *33*, 889.
(67) Chen, H. L.; Wang, S. F.; Lin, T. L. *Macromolecules* **1998**, *31*, 8924.
(68) Chen, H. L.; Li, L. J.; Lin, T. L. *Macromolecules* **1998**, *31*, 2255.
(69) Runt, J.; Zhang, X.; Miley, D. M.; Gallagher, K. P.; Zhang, A. *Macromolecules* **1992**, *25*, 3902.
(70) Hoffman, J. D.; Weeks, J. J. *J. Chem. Phys.* **1965**, *42*, 4301.
(71) Chiu, H. J.; Chen, H. L.; Lin, T. L.; Lin, J. S. *Macromolecules* **1999**, *32*, 4969.
(72) Shieh, Y. T.; Lin, Y. G.; Chen, H. L. *Polymer* **2002**, *43*, 3691.
(73) Irionod, P.; Iruin, J. J.; Fernandex-Berridi, M. J. *Macromolecules* **1996**, *29*, 5605.
(74) Chen, H. L.; Liu, H. H.; Lin, J. S. *Macromolecules* **2000**, *33*, 4856.
(75) Kuo, S. W.; Lin, C. L.; Chang, F. C. *Macromolecules* **2002**, *35*, 278.
(76) Zhang, L. L.; Goh, S. H.; Lee, S. Y. *J. Appl. Polym. Sci.* **1998**, *70*, 1811.
(77) Coleman, M. M.; Yang, X.; Zhang, H.; Painter, P. C. *J. Macromol. Sci., Phys.* **1993**, *B32*, 295.

MA034695A